JACS
JOURNAL OF THE AMERICAN CHEMICAL SOCIETY

Article

pubs.acs.org/JACS

First-Principles Calculation of Dielectric Response in Molecule-Based Materials

Henry M. Heitzer, Tobin J. Marks,* and Mark A. Ratner*

Department of Chemistry and the Materials Research Center, Northwestern University, 2145 Sheridan Road, Evanston Illinois 60208, United States

Supporting Information

ABSTRACT: The dielectric properties of materials are of fundamental significance to many chemical processes and the functioning of numerous solid-state device technologies. While experimental methods for measuring bulk dielectric constants are well-established, far less is known, either experimentally or theoretically, about the origin of dielectric response at the molecular/multimolecular scale. In this contribution we report the implementation of an accurate first-principles approach to calculating the dielectric response of molecular systems. We assess the accuracy of the method by reproducing the experimental dielectric constants of several bulk π-electron materials and demonstrating the ability of the method to capture dielectric properties as a function of frequency and molecular orientation in representative arrays of substituted aromatic derivatives. The role of molecular alignment and packing density on dielectric response is also examined, showing that the local dielectric behavior of molecular assemblies can diverge significantly from that of the bulk material.

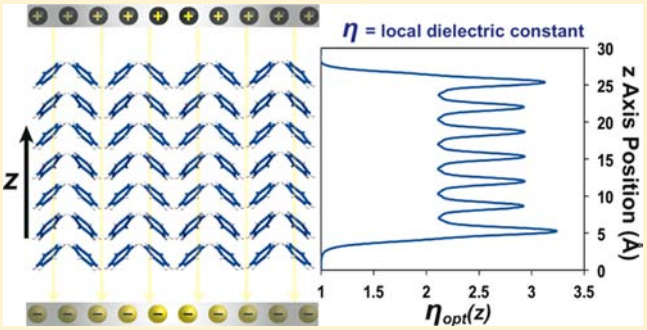

INTRODUCTION

The dielectric properties of molecule-based materials are critical to a host of important scientific phenomena, including enzyme function,[1−3] electron transfer,[4−6] chemical sensors,[7−10] and an array of electronics applications,[11−14] such as in nanoscale self-assembled dielectric materials for gating thin-film transistors,[15−18] as well as in thin interfacial extraction/blocking layers for organic light-emitting diodes and photovoltaic cells.[19−21] The dielectric constant expresses the quantity of electrical energy that can be stored in a particular material under an applied field and is significantly materials-, frequency-, and temperature-dependent. Experimentally, the frequency and temperature dependences of the dielectric constants of numerous bulk materials have been thoroughly characterized and tabulated.[22] However, little focus,[23−29] either theoretical or experimental, has been devoted to understanding the dielectric properties of organic materials at the molecular scale as a prelude to describing the dielectric response of multimolecular arrays.

The capability to accurately model and efficiently predict molecular scale dielectric response should help guide the design of new high and low dielectric constant materials and enable the tailoring of desired dielectric characteristics for specific applications. Independent of material design, understanding the dielectric environment would help elucidate mechanisms in a wide array of chemical processes.[30−35] In this report we present a first-principles approach to computing the dielectric constants of molecular systems, beginning at the atomistic level, and permitting the relationships between specific chemical bonding arrangements and their dielectric response to be accurately described. This contribution is organized as follows: we first present the general framework of the methodology, then address three essential concepts related to the dielectric response of molecule-based systems, (1) frequency dependence, (2) role of molecular orientation, and (3) relationship to molecular packing.

The approach taken here for computing the dielectric response of a molecular material measures the change in charge density as a function of applied electric field.[36,37] We focus first on monolayers of molecules, to ascertain the variance of the local dielectric response at different locations along a specific molecular axis. The electric field is applied along the molecular axis perpendicular to the substrate surface in which the monolayers lie; this axis will be referred to as the z axis. In this study, all of the molecules are aligned parallel to one another, with the centers of mass located at the same z coordinate in space, as shown in Figure 1. The calculations use the plane wave DFT program, QUANTUM ESPRESSO,[38] consequently the material is treated as periodic in the plane (xy plane) perpendicular to the electric field. The local dielectric constant computed at each z coordinate is thus averaged over the xy plane of the entire unit cell, providing a planar-averaged local dielectric response that varies as a function of molecular architecture along the z-axis.

Received: February 21, 2013
Published: June 4, 2013

   dx.doi.org/10.1021/ja401904d | J. Am. Chem. Soc. 2013, 135, 9753−9759

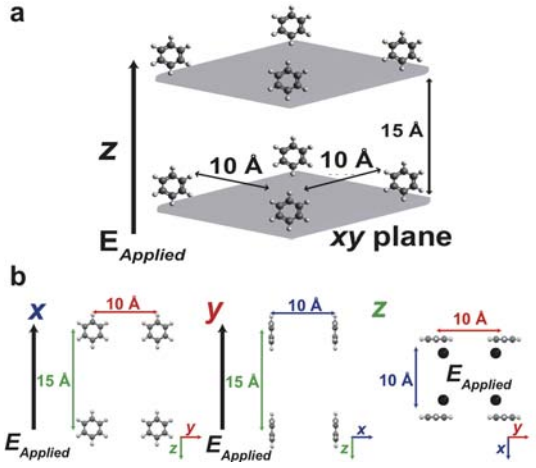

Figure 1. Coordinate system used for first-principles DFT calculation of the optical and static dielectric response of aromatic molecular arrays. Diagram of a 2 × 2x2 simulation cell for a benzene monolayer (a) and orientations of the benzene molecules looking down the *x*, *y*, and *z* axes (b). The *z* axis is parallel to the applied electric field. The simulation cell is periodic in all 3 directions, but the large vacuum along the *z* axis insures that the monolayers do not interact.

The planar-averaged local dielectric constant, which is called $\eta(z)$ here, provides two informative quantities in monolayer systems. First, once the local dielectric response along a particular molecular direction (i.e., at a specific *z* coordinate) is known, a direct comparison between specific structural features and the corresponding dielectric response can be performed. Second, while $\eta(z)$ is a nonmeasurable quantity, by applying a parallel plate capacitor model[39] the experimentally observable dielectric constant ε can be computed using eq 1.

$$\frac{a-b}{\varepsilon} = \sum_{i=a}^{b} \frac{1}{\eta_i} \tag{1}$$

Here, η_i is the calculated local dielectric constant at a given index *i* along the *z* coordinate, the *a* and *b* indices correspond to the origin and terminus of the molecule, respectively, and ε is the dielectric constant averaged over the length of the molecule. Here the origin and terminus of the molecule are defined as the positions along the *z*-axis of the lowermost and uppermost constituent atoms, respectively. The dielectric constant ε is formally the permittivity $A(\omega)$, defined by $\varepsilon(\omega) = \varepsilon_0 A(\omega)$. A more detailed description of the computational technique used here can be found in the Supporting Information (SI). Details about the specific computational input parameters can be found in the Computational Methodology section below. By applying this scheme to several simple systems, the capability to model accurately the dielectric response in multimolecular systems is demonstrated, and important trends governing molecular dielectric response are deduced.

COMPUTATIONAL METHODOLOGY

The general calculation procedure is as follows. The system is first relaxed in the absence of an electric field, in the corresponding packing arrangement of interest. In the monolayer systems discussed here, each molecule is separated by 10 Å in the *x* and *y* directions, and 15 Å of vacuum along the *z* the axis is introduced to ensure minimal interaction between the monolayers. Demonstration that this vacuum separation is sufficient to ensure negligible interaction can be found in the SI. Information about the crystalline benzene system can be found below. After the system is relaxed, two electric fields ($E_{applied}$), ± 0.001 au, are applied parallel to the *z* axis. Smaller fields were also applied and induced negligible variation in optical dielectric profile and only minor changes in the static dielectric profile (see SI). The 3D charge density profile is then generated, and subsequently a planar average is taken for each along the *z* axis. $\overline{\rho}_{ind}(z)$, the difference in the charge density profiles at the different electric field strengths, is related to the induced polarization, $\overline{\rho}(z)$, using eq 2.

$$\frac{d}{dz}\overline{p}(z) = -\overline{\rho}_{ind}(z) \tag{2}$$

The induced polarization is then used to calculate the local dielectric constant, $\eta(z)$ (eq 3),

$$\eta(z) = \frac{\varepsilon_0 E_{ext}}{\varepsilon_0 E_{ext} - \overline{P}(Z)} \tag{3}$$

with ε_0 the vacuum permittivity divided by 4π, and $E_{ext} = 2 \times E_{applied}$. In this contribution, E_{ext} = 0.002 au A full derivation of this relationship can be found in the SI. The optical dielectric constant where $\omega \to \infty$ is calculated assuming that only the electrons respond to the electric field (i.e., optical regime). The static dielectric constant where $\omega \to 0$ is calculated by allowing the internal molecular geometry to relax in the presence of an electric field. In both the optical and static response, no translational or rotational motion is allowed. In terms of computational demands, the local static dielectric constant is more computationally intensive due to the geometry optimization required versus a single-point calculation for the local optical dielectric constant. The calculations were performed using DFT within the local density approximation (LDA) using the Perdew–Zunger (PZ) parametrization[40] and Vanderbilt ultrasoft pseudopotentials,[41] as implemented in QUANTUM ESPRESSO.[38] An evaluation of the functional choice was performed, examining the generalized gradient approximation (GGA) as implemented by the Perdew–Burke–Ernzerhof (PBE)[42] functional and a range-separated hybrid functional Heyd–Scuseria–Ernzerhof 06 (HSE06).[43] In the case of HSE06, norm-conserving pseudopotentials were used. Little variation in the dielectric profiles is noted among the chosen functionals. The dielectric profiles of benzene using the PZ, PBE, and HSE06 functionals are provided in the SI. Unless otherwise stated, forces were relaxed to 9 meV/Å and a 1 × 2 × 2 k-point point scheme was used to sample the Brillioun Zone (BZ) in calculations. The wave functions and the augmented charge density are represented by plane-wave basis sets with energy cutoffs of 60 and 720 Ry, respectively. Geometries and energies of the molecules used in this study are given in the SI.

To model bulk benzene, slabs of crystalline benzene 23 Å thick along the *z* axis were constructed. The lattice parameters are as follows: $\alpha = \beta = \gamma = 90°$, *a* = 38.000 Å, *b* = 9.201 Å, *c* = 6.690 Å (*a* here corresponds to the *z* axis, *b* to the *y* axis and *c* to the *x* axis). The supercell was created using benzene crystal structure data[44] and subsequently deleting 15 Å of benzene along the *z* axis. This creates an orthorhombic supercell containing an infinite slab of benzene in the *x* and *y* directions separated by 15 Å of vacuum in the *z* direction. Similarly, bulk 1,3-dinitrobenzene was modeled using a crystalline slab 31 Å thick along the *z* axis using crystal structure data.[45] The lattice parameters are as follows $\alpha = \beta = \gamma = 90°$, *a* = 46.000 Å, *b* = 13.292 Å, *c* = 3.802 Å. The coordinates for all atoms in both bulk systems are given in the SI.

RESULTS AND DISCUSSION

Frequency Dependence of the Dielectric Response. Different contributions to the dielectric response of a molecular material are evident at distinct frequencies of the applied electric field.[46] In the low-frequency regime, geometric rearrangements/oscillations can contribute to large dielectric responses, while at high frequencies, only the electronic response is important since only electrons can respond to the rapidly oscillating electric field. These contributions and their

dx.doi.org/10.1021/ja401904d | J. Am. Chem. Soc. 2013, 135, 9753–9759

corresponding frequency dependences are often critical determinants of the dielectric constant of a material. For example, at low frequencies water has a dielectric constant of 78.6,[47] while at high frequencies, where the dipoles cannot reorient rapidly in response to the oscillating field, the dielectric constant falls to 1.7.[48] It is therefore important that a useful theoretical description be able to differentiate between these frequency regimes and to describe the dielectric response across a broad range of frequencies.

In this report we focus on two frequency regimes. In the high frequency limit, $\omega \rightarrow \infty$, described by the optical dielectric constant, only the electrons are allowed to relax in the presence of the electric field while the nuclear coordinates are held fixed. In the low frequency limit, $\omega \rightarrow 0$, described by the static dielectric constant, internal geometric reorganization is allowed by permitting displacements of the nuclei. In both frequency regimes, no overall molecular translational or rotational motion is allowed; only internal molecular motions that do not translate the center of mass or effect rotation about molecular axes are permitted. Indeed, such internal motions constitute the difference between what will be called ε_{static} and $\varepsilon_{optical}$. As the water example shows, translations and rotations induce very large changes in ε . Since we deal here with only solids and films, this definition of ε_{static} is adequate. To model fluid systems, one would have to account for these translational and rotational processes in order to accurately capture the dielectric response. To verify that the present approach accurately captures the frequency dependence of molecular systems, sparsely packed (1 molecule/nm^2) periodically spaced monolayers of benzene, fluorobenzene, and chlorobenzene molecules are first examined. These test molecular monolayers were chosen because of their simplicity and the dissimilarities that should exist in their static and optical dielectric responses. The sparse surface coverage insures that essentially no significant intermolecular interactions take place and obviously does not represent an experimentally accessible molecular monolayer regime at this stage of the analysis. Taking the planar average of the charge density in these sparse systems removes any dependence on the molecular orientation with respect to the z axis, i.e. the dielectric response is invariant to rotation about the z axis.

In general, high-frequency dielectric response is primarily determined by the atomic radius and the density of the constituent atoms comprising a molecule.[49,50] Correspondingly, it might be expected that the optical dielectric responses of benzene and fluorobenzene would be similar due to the similar atomic radii of the H and F atoms, while chlorobenzene might have a significantly greater response. Figure 2a details the computed optical dielectric response of three monolayers composed of these three molecules. The optical dielectric response computed with this technique is in good agreement with basic chemical intuition. Thus, the local dielectric constant is similar across the three molecules until the z coordinate reaches the point of differing substitution. At this site, benzene and fluorobenzene exhibit nearly identical optical dielectric responses, whereas chlorobenzene exhibits a markedly greater response.

Note that the bulk static dielectric constant is an average over all different molecular orientations and polarizations. Since we are modeling a sparse monolayer system and not permitting molecular rotation or translation, negligible geometric reorganization occurs—as discussed above, this component dominates in most liquids and gases having thus been a combination of the

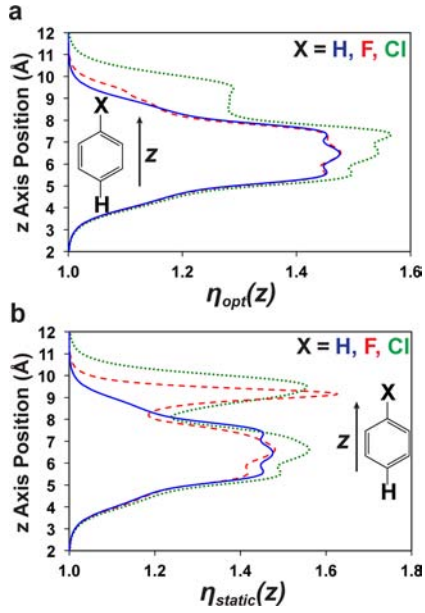

Figure 2. Computed local optical (a) and static (b) dielectric constant of a monolayer of benzene (solid), fluorobenzene (dashed), and chlorobenzene (dotted). There is an imposed 10 Å separation in x and y directions between each molecule. The applied electric field is parallel to the z axis and has a strength of ±0.001 au, and the response is averaged over the xy plane.

electronic/optical dielectric response and any additional polarization provided by intramolecular nuclear motion involving polar bonds. Since benzene has little polar bonding, the static dielectric response is expected to be nearly identical to the optical response. However, for fluorobenzene and chlorobenzene, there should be variations caused by the oscillations of the polar carbon−halogen bonds. Figure 2b details the static dielectric response of the three materials. As anticipated, for benzene, the static and optical dielectric constants are indistinguishable. The local optical and static dielectric responses for each material are given in the SI. In contrast, the halogenated benzenes contain polar bonds and consequently have different static and optical dielectric responses, primarily differing in the vicinity of the carbon−halogen bond, as evident in Figure 2b. In modeling the optical and static dielectric response of these molecular layers, it is evident that the present approach is capable of (a) correlating chemical functional groups to specific dielectric responses and (b) discerning different dielectric responses based on the frequency regime of the applied field.

Orientational Dependence of the Dielectric Response. The previous section examined a sparse monolayer at a single molecular orientation. In real systems the dielectric response is typically measured over an ensemble of orientations and displacements for a given density of the material. To examine how molecular orientation affects the dielectric response, the benzene molecule presented in the previous section is now rotated such that the molecular plane lies perpendicular to the applied electric field. The parallel and perpendicular alignments with the corresponding static dielectric responses are shown in Figure 3. The dielectric response is found here to be markedly different in the parallel and perpendicular orientations. Note that the benzene orientation parallel to the field has a more delocalized response due to the greater π-system extension

dx.doi.org/10.1021/ja401904d | J. Am. Chem. Soc. 2013, 135, 9753−9759

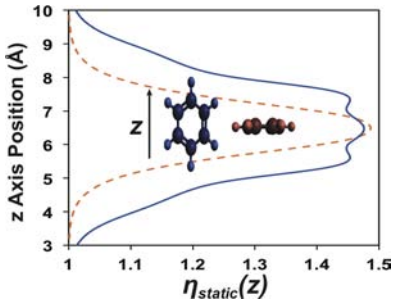

Figure 3. Local static dielectric constant of a monolayer of benzene with the π-plane oriented parallel (solid) and perpendicular (dashed) to the electric field. For clarification, it is the individual benzene molecules comprising the monolayers that are oriented parallel or perpendicular to the electric field. There is an imposed 10 Å separation in x and y directions between each molecule. The applied electric field is parallel to the z axis and has a strength of ±0.001 au, and the response is averaged over the xy plane.

along the z axis and exhibits greater polarization versus the perpendicular benzene orientation.

Both orientations have the largest dielectric responses at the center of the benzene molecule, with little disparity in the maximum response (η_{max} = 1.43 for the parallel, η_{max} = 1.47 for the perpendicular orientation). However, due to the breadth of the dielectric response in the parallel orientation, computing the dielectric constant over the entirety of the parallel benzene ring using eq 1 yields an overall dielectric constant for the parallel orientation which is larger than in the perpendicular orientation ($\varepsilon_{\parallel}$ = 1.32 vs $\varepsilon_{\perp}$ = 1.17). This result demonstrates the importance of molecular orientation on the dielectric response of a material. In fully disordered bulk macroscopic media this anisotropy is unimportant, since all orientations are represented and averaged in a standard dielectric measurement. Conversely, when studying processes at the nanoscale, the polarization response of a single molecule in a specific orientation may be important in a variety of chemical and physical processes.[51,52] For example, in self-assembled molecular monolayers, where the orientations of the molecular components can be controlled, this information should be useful for designing in specific dielectric responses for a given molecular assembly.[53,54] This effect is also seen when measuring the dielectric response of crystalline materials, which may exhibit anisotropic dielectric responses depending on the direction of the applied field.[55−57] Thus, the local dielectric response of a molecule is not determined solely by chemical composition, but critically influenced by the orientation of the molecule with respect to the applied electric field.

Molecular Density Dependence of the Dielectric Response. Thus far, only a sparse molecular surface coverage has been examined, imposing low molecular densities in the materials being studied. This low coverage contributes to the smaller than intuitively expected computed dielectric constants, varying from ε = 1.0−1.8, as discussed above, while the bulk dielectric constant of frozen benzene is reported to be 2.34.[58] To next investigate how the dielectric response of a material varies with molecular density, the packing density of a benzene monolayer was increased to 2, 3, and 4 times the original density of 1 mol/nm^2. Figure 4 shows that the static dielectric response increases essentially linearly with packing density. This result highlights the importance of molecular density in dielectric materials design since it greatly alters the response.

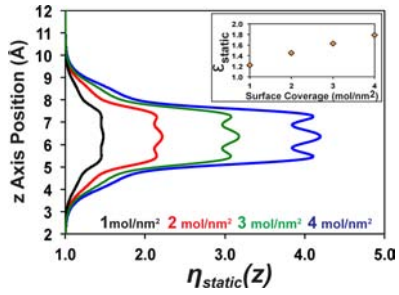

Figure 4. Computed local static dielectric constant of a monolayer of benzene at different packing densities: 1 (black), 2 (red), 3 (green), and 4 (blue) mol/nm^2. The inset shows the calculated static dielectric constant as a function of packing density. There is an imposed intermolecular separation distance, 10 Å, 7.07 Å, 5.74 Å, or 5 Å for the respective packing densities in ascending order, in x and y directions between each molecule. The applied electric field is parallel to the z axis and has a strength of ±0.001 au, and the response is averaged over the xy plane.

To verify the accuracy of the present technique in computing the dielectric response of multimolecular materials, a 23 Å thick slab of benzene molecules, with coordinates taken from the benzene crystal structure,[44] was next analyzed. Figure 5a shows

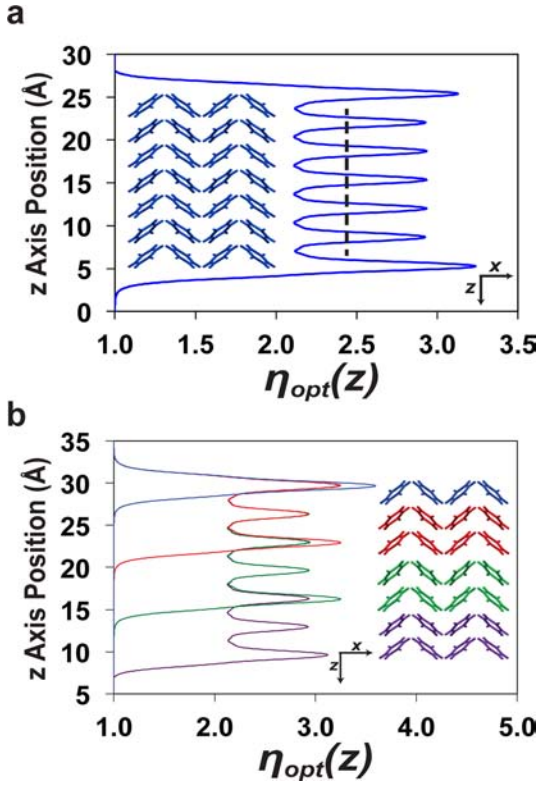

Figure 5. The local optical dielectric constant of seven benzene layers (a) and at different thicknesses: 1 (blue), 3 (red), 5 (green), and 7 (purple) benzene layers (b) along the z axis. The images next to the dielectric response are xz cross sections of the benzene crystal structure slabs looking down the y axis. The exact benzene crystal structure is given in the SI. Note that the benzene is infinitely repeated in the x and y directions using periodic boundary conditions. The dashed line in Figure 5a represents the region considered to be bulk, i.e., with minimal surface effects. The electric field is applied parallel to the z axis and has a strength of ±0.001 au, and the response is averaged over the xy plane.

dx.doi.org/10.1021/ja401904d | J. Am. Chem. Soc. 2013, 135, 9753−9759

the benzene slab and the computed optical dielectric response. Only the local optical dielectric constant is examined here since, as discussed above, the optical and static dielectric constants are essentially equivalent in benzene. In the previous section, the importance of molecular orientation on the dielectric response was demonstrated. The molecular orientation and density is different when viewed down each axis, requiring the dielectric response along the other two axes to also be computed. The dielectric profile along the x and y axes and unit cell information can be found in the SI. No information about the molecular orientation was reported in ref 54. We assume that the measurement was taken on a polycrystalline sample of frozen benzene. The dielectric constant along each axis is calculated from eq 1 with $\varepsilon_z = 2.39$, $\varepsilon_y = 2.69$, $\varepsilon_x = 2.33$, respectively. Taking the theoretical dielectric constant as the average of these three values we find excellent agreement between the theoretical bulk dielectric constant ($\varepsilon_{theory} = 2.46$) and the experimental dielectric constant ($\varepsilon_{exp} = 2.34$).[58] The crystalline bulk is defined as the region in which the dielectric response repeats periodically and is indicated in Figure 5a by the dashed line. These results demonstrate the excellent accuracy of the present computational approach, highlighting the importance of molecular density in determining the bulk dielectric constant. Also of note is the rapid convergence of the local dielectric constant to a bulk response, requiring only a single layer of benzene to effectively eliminate any effects of the vacuum surface on the dielectric response of the material. The dielectric response as a function of benzene slab thickness is given in Figure 5b, which shows that the internal (i.e., first noninterfacial layer) local dielectric constant is independent of slab thickness.

Benzene provides an excellent test case for a nonpolar molecule. To examine how the present method performs on polar substances we chose 1,3-dinitrobenzene and performed the same analysis on a 35 Å slab using coordinates taken from 1,3-dinitrobenzene crystal structure.[48] Since there are polar bonds in 1,3-dinitrobenzene we would expect a deviation between the static and optical responses. To accelerate convergence, the first layer on either side of the slab was fixed. Since the initial layer has little effect on the bulk behavior, as shown in benzene, it is reasonable to assume that this will not have a significant effect on the 1,3-dinitrobenzene dielectric response. Additionally the force convergence threshold was increased to 13 meV/Å. When tested on a smaller cluster of dinitrobenzene molecules, there was no change in the static or optical dielectric response. Freezing of the initial layer and increasing the force threshold was performed to decrease the initial geometry convergence time, which was considerable for a system of this size. Figure 6 shows the 1,3-dinitrobenzene slab and the computed optical and static dielectric response. As in benzene, the crystal structure of 1,3-dinitrobenzene has different molecular orientations and densities when viewed down each axis, requiring calculations along the other two axes. The dielectric profiles along the x and y axes can be found in the SI. The optical dielectric constant along each axis is calculated using eq 1 with ε_z^{opt} =2.79, $\varepsilon_y^{opt} = 2.92$, $\varepsilon_x^{opt} = 2.07$. The static dielectric constant along each axis is calculated using eq 1 with $\varepsilon_z^{static} = 3.13$, $\varepsilon_y^{static} = 3.91$, $\varepsilon_x^{static} = 2.07$ Taking the averages we obtain values of $\varepsilon_{theory}^{opt} = 2.59$ and $\varepsilon_{theory}^{static} = 3.05$ for the optical and static dielectric constants respectively. The reported dielectric constant for 1,3-dinitrobenzene is $\varepsilon_{exp} = 2.85$ at an applied frequency 4×10^8 Hz.[58] At this frequency, the polar bonding will contribute to the dielectric response making

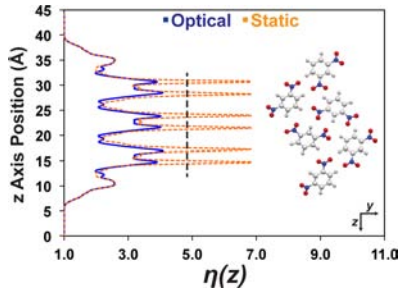

Figure 6. Computed local optical (solid blue) and static (dashed orange) dielectric constant of 1,3-dinitrobenzene. The exact crystal structure is given in the SI The image next to the dielectric response is the xz cross-section of the 1,3-dinitrobenzene crystal structure slab viewed down the y axis. Note that the 1,3-dinitrobenzene is infinitely repeated in the x and y directions using periodic boundary conditions. The dashed line in a represents the region considered to be bulk, i.e., with minimal surface effects. The electric field is applied parallel to the z axis and has a strength of ±0.001 au, and the response is averaged over the xy plane.

the calculated static dielectric constant the value to compare to experiment. The experimental and computed dielectric constants are in good agreement, showing the validity of this method on polar materials. As found for benzene there is rapid convergence to bulk properties for both the static and optical dielectric behavior in this polar material. Similar results are reported in inorganic materials, with surface effects from vacuum and nonhomogenous systems vanishing within a nm.[37]

Previous attempts to model molecular/multimolecular dielectric behavior relied on classical descriptions such as the Clausius−Mossotti or Lorentz−Lorenz models to relate the molecular polarizabilities in vacuum to bulk dielectric constants.[59] However, as shown by Vanderbilt et al.,[60] these relationships, while valid in some scenarios, are inappropriate for many materials because classical theories require polarization be partitioned into localized centers. In real materials the induced charge is delocalized, making any partition largely arbitrary. These classical approaches also rely on combining a molecular response (polarizability) with a bulk property (density) in order to estimate the corresponding dielectric response. In contrast, the technique presented here is ideal for molecule-based systems because it directly ties the electronic response of the material (the change in charge density) to the specifics of molecular orientations and packing by implementing the periodic boundary conditions of plane wave DFT. These results also demonstrate the inadequacy of starting from a concept such as the dielectric constant of a single molecule, because the actual measured ε is in fact a bulk, ensemble property dependent on the arrangement and packing motif of the constituent molecules.

The present results illustrate how the dielectric behavior of a material varies even at the single-molecule level. Thus, there can be dramatically different dielectric responses in chemical systems upon varying the position, orientation, and packing density of the constituent molecules. We stress the concept of a *local* dielectric response where the dielectric characteristics of a material over a given length scale may be substantially different from those of the bulk material. This *local* dielectric response should be taken into account when both evaluating and designing electrostatic interactions in molecular-scale systems, since under some conditions (especially at the nanoscale) the bulk dielectric constant may not accurately describe the

dielectric behavior at the location of interest. For example, when creating a self-assembled monolayer of conjugated organic molecules to use as gate dielectrics it would be advantageous to align the constituent molecules such that the applied field is parallel to the π system. While a random distribution of molecular orientations might result in a low dielectric constant, by ordering the molecules such that the polarizable π system is parallel with the applied field a high dielectric constant can be achieved. This molecular ordering may explain why self-assembled nanodielectrics (SANDs),[15,53,61,62] whose π systems are predominately parallel to the applied field, achieve such large dielectric constants, $\varepsilon >$ 9.00, while almost all other solid state organic materials have a ε < 4.00. It is also foreseeable to use this technique for materials design by determining structure−function relationships describing those molecular properties leading to large dielectric responses by examining the local dielectric behavior of test molecules to pinpoint regions with the largest dielectric response.

CONCLUSIONS

An approach is reported here to model the dielectric response of molecule-based materials. By analyzing molecular monolayers at varying packing densities and molecular alignments, the diverse contributions to the dielectric response at the low and high frequency limits are elucidated. Altering the alignment of the molecules effects a significant change in the dielectric response, highlighting the importance of molecular orientation on the bulk dielectric constant. By examining both polar and nonpolar bulk systems, the accuracy of this technique is demonstrated and the effect of molecular density on the dielectric response is elucidated. This methodology thus offers the capability to analyze and accurately predict the dielectric response of large molecular systems while still capturing important *local* dielectric properties. Due to the importance of the dielectric response of materials in many electronic and opto-electronic systems, this technique should provide a powerful and informative guide for materials design.

ASSOCIATED CONTENT

Supporting Information

Detailed derivation of technique, functional dependence, comparison of static and optical dielectric response, effect of the electric field strength on the dielectric response, interaction between molecules, dielectric calculations along the x and y axes for benzene and 1,3-dinitrobenzene, geometry and energies of molecules used in this study and crystal structure information used. This material is available free of charge via the Internet at http://pubs.acs.org.

AUTHOR INFORMATION

Corresponding Author

t-marks@northwestern.edu (T.J.M.); ratner@northwestern.edu (M.A.R.).

Notes

The authors declare no competing financial interest.

ACKNOWLEDGMENTS

The research was supported by the MRSEC program of NSF (DMR-1121262) through the Northwestern University Materials Research Center. H.M.H. is supported by the Department of Defense (DoD) through the National Defense Science & Engineering Graduate Fellowship (NDSEG) Program. H.M.H. thanks S. Parker, S. Roy, B. Savoie, M. Blaber, and A. Nitzan for insightful discussions.

REFERENCES

(1) Mertz, E. L.; Krishtalik, L. I. *Proc. Natl. Acad. Sci. U.S.A.* **2000**, *97*, 2081−2086.
(2) Dudev, T.; Lim, C. *J. Phys. Chem. B* **2000**, *104*, 3692−3694.
(3) Hernández, G.; Anderson, J. S.; LeMaster, D. M. *Biochemistry* **2009**, *48*, 6482−6494.
(4) Roth, J. P.; Klinman, J. P. *Proc. Natl. Acad. Sci. U.S.A.* **2003**, *100*, 62−67.
(5) Marcus, R. A. *J. Electroanal. Chem.* **1997**, *438*, 251−259.
(6) Maroncelli, M.; Macinnis, J.; Fleming, G. R. *Science* **1989**, *243*, 1674−1681.
(7) Hagleitner, C.; Hierlemann, A.; Lange, D.; Kummer, A.; Kerness, N.; Brand, O.; Baltes, H. *Nature* **2001**, *414*, 293−296.
(8) Mannsfeld, S. C. B.; Tee, B. C.-K.; Stoltenberg, R. M.; Chen, C. V. H.-H.; Barman, S.; Muir, B. V. O.; Sokolov, A. N.; Reese, C.; Bao, Z. *Nat. Mater.* **2010**, *9*, 859−864.
(9) Sokolov, A. N.; Tee, B. C.-K.; Bettinger, C. J.; Tok, J. B.-H.; Bao, Z. *Acc. Chem. Res.* **2012**, *45*, 361−371.
(10) Sherry, L. J.; Chang, S.-H.; Schatz, G. C.; Van Duyne, R. P.; Wiley, B. J.; Xia, Y. *Nano Lett.* **2005**, *5*, 2034−2038.
(11) Newaz, A. K. M.; Puzyrev, Y. S.; Wang, B.; Pantelides, S. T.; Bolotin, K. I. *Nat. Commun* **2012**, *3*, 734.
(12) Ortiz, R. P.; Facchetti, A.; Marks, T. J. *Chem. Rev.* **2010**, *110*, 205−239.
(13) Zotti, G.; Vercelli, B.; Berlin, A. *Acc. Chem. Res.* **2008**, *41*, 1098−1109.
(14) Vilan, A.; Yaffe, O.; Biller, A.; Salomon, A.; Kahn, A.; Cahen, D. *Adv. Mater. Weinheim* **2010**, *22*, 140−159.
(15) Yoon, M.-H.; Kim, C.; Facchetti, A.; Marks, T. J. *J. Am. Chem. Soc.* **2006**, *128*, 12851−12869.
(16) Klauk, H.; Zschieschang, U.; Pflaum, J.; Halik, M. *Nature* **2007**, *445*, 745−748.
(17) Weitz, R. T.; Zschieschang, U.; Forment-Aliaga, A.; Kälblein, D.; Burghard, M.; Kern, K.; Klauk, H. *Nano Lett.* **2009**, *9*, 1335−1340.
(18) DiBenedetto, S. A.; Facchetti, A.; Ratner, M. A.; Marks, T. J. *J. Am. Chem. Soc.* **2009**, *131*, 7158−7168.
(19) Hotchkiss, P. J.; Li, H.; Paramonov, P. B.; Paniagua, S. A.; Jones, S. C.; Armstrong, N. R.; Brédas, J.-L.; Marder, S. R. *Adv. Mater.* **2009**, *21*, 4496−4501.
(20) Brédas, J.-L.; Norton, J. E.; Cornil, J.; Coropceanu, V. *Acc. Chem. Res.* **2009**, *42*, 1691−1699.
(21) Veinot, J.; Marks, T. J. *Acc. Chem. Res.* **2005**, *38*, 632−643.
(22) Von Hippel, A. R. In *Dielectric Materials and Applications*; Von Hippel, A. R., Ed.; Artech House: Boston, MA, 1995.
(23) Romaner, L.; Heimel, G.; Ambrosch-Draxl, C.; Zojer, E. *Adv. Funct. Mater.* **2008**, *18*, 3999−4006.
(24) Natan, A.; Kuritz, N. *Adv. Funct. Mater.* **2010**, *20*, 2077−2084.
(25) Shi, N.; Ramprasad, R. *Phys. Rev. B* **2006**, *74*, 045318.
(26) Ellenbogen, J. C.; Picconatto, C. A. *Phys. Rev. A* **2007**, *75*, 042102.
(27) Smith, F. T. *J. Chem. Phys.* **1961**, *34*, 793−801.
(28) Jensen, L.; Aastrand, P.-O.; Mikkelsen, K. V. *Int. J. Quantum Chem.* **2001**, *84*, 513−522.
(29) Sabin, J. R.; Trickey, S. B.; Apell, S. P. *Int. J. Quantum Chem.* **2000**, *77*, 358−366.
(30) Nymeyer, H.; Zhou, H.-X. *Biophys. J.* **2008**, *94*, 1185−1193.
(31) Hyun, B.-R.; Bartnik, A. C.; Lee, J.-K.; Imoto, H.; Sun, L.; Choi, J. J.; Chujo, Y.; Hanrath, T.; Ober, C. K.; Wise, F. W. *Nano Lett.* **2010**, *10*, 318−323.
(32) Venkatesh, M. S.; Raghavan, G. S. V. *Biosyst. Eng.* **2004**, *88*, 1−18.
(33) Schutz, C. N.; Warshel, A. *Proteins* **2001**, *44*, 400−417.
(34) Mahmoud, M. A.; Chamanzar, M.; Adibi, A.; El-Sayed, M. A. *J. Am. Chem. Soc.* **2012**, *134*, 6434−6442.

(35) Tomasi, J.; Mennucci, B.; Cammi, R. *Chem. Rev.* **2005**, *105*, 2099−3093.
(36) Giustino, F.; Pasquarello, A. *Phys. Rev. B* **2005**, *71*, 144104.
(37) Yu, L.; Ranjan, V.; Nardelli, M.; Bernholc, J. *Phys. Rev. B* **2009**, *80*, 165432.
(38) Giannozzi, P.; Baroni, S.; Bonini, N.; Calandra, M.; Car, R.; Cavazzoni, C.; Ceresoli, D.; Chiarotti, G. L.; Cococcioni, M.; Dabo, I.; Dal Corso, A.; de Gironcoli, S.; Fabris, S.; Fratesi, G.; Gebauer, R.; Gerstmann, U.; Gougoussis, C.; Kokalj, A.; Lazzeri, M.; Martin-Samos, L.; Marzari, N.; Mauri, F.; Mazzarello, R.; Paolini, S.; Pasquarello, A.; Paulatto, L.; Sbraccia, C.; Scandolo, S.; Sclauzero, G.; Seitsonen, A. P.; Smogunov, A.; Umari, P.; Wentzcovitch, R. M. *J. Phys.: Condens. Matter* **2009**, *21*, 395502.
(39) Sze, S. M.; Lee, M.-K. *Semiconductor Devices: Physics and Technology*; Wiley: New York, NY, 2002.
(40) Zunger, A.; Perdew, J. P.; Oliver, G. L. *Solid State Commun.* **1980**, *34*, 933−936.
(41) Vanderbilt, D. *Phys. Rev. B* **1990**, *41*, 7892−7895.
(42) Perdew, J.; Burke, K.; Ernzerhof, M. *Phys. Rev. Lett.* **1996**, *77*, 3865−3868.
(43) Krukau, A. V.; Vydrov, O. A.; Izmaylov, A. F.; Scuseria, G. E. *J. Chem. Phys.* **2006**, *125*, 224106.
(44) Budzianowski, A.; Katrusiak, A. *Acta Crystallogr., Sect. B* **2006**, *62*, 94−101.
(45) Wójcik, G.; Mossakowska, I.; Holband, J.; Bartkowiak, W. *Acta Crystallogr., Sect. B* **2002**, *58*, 998−1004.
(46) Scaife, B. K. P. *Principles of Dielectrics*; Oxford University Press: New York, 1998.
(47) Drake, F.; Pierce, G.; Dow, M. *Phys. Rev.* **1930**, *35*, 613−622.
(48) Hale, G. M.; Querry, M. R. *Appl. Opt.* **1973**, *12*, 555−563.
(49) Lipkin, M. R.; Martin, C. C. *Ind. Eng. Chem. Res.* **1946**, *18*, 380−381.
(50) Sharma, P.; Katyal, S. C. *J. Appl. Phys.* **2010**, *107*, 113527.
(51) Dressel, M.; Gompf, B.; Faltermeier, D.; Tripathi, A. K.; Pflaum, J.; Schubert, M. *Opt. Express* **2008**, *16*, 19770−19778.
(52) Li, H.; Li, W.; Feng, Y.; Liu, J.; Pan, H.; Zeng, H. *Phys. Rev., A* **2012**, *85*, 052515.
(53) Yoon, M. H. *Proc. Natl. Acad. Sci. U.S.A.* **2005**, *102*, 4678−4682.
(54) DiBenedetto, S. A.; Facchetti, A.; Ratner, M. A.; Marks, T. J. *Adv. Mater.* **2009**, *21*, 1407−1433.
(55) Zang, D. Y.; So, F. F.; Forrest, S. R. *Appl. Phys. Lett.* **1991**, *59*, 823.
(56) Cho, T. H.; Lee, J. K.; Ho, P. S.; Ryan, E. T.; Pellerin, J. G. *J. Vac. Sci. Technol. B* **2000**, *18*, 208.
(57) Dey, S.; Pal, A. J. *Langmuir* **2011**, *27*, 8687−8693.
(58) National Research Council. In *International Critical Tables of Numerical Data, Physics, Chemistry and Technology*; Washburn, E. W., Ed.; McGraw-Hill: New York, NY, 1928.
(59) Blythe, A. R.; Bloor, D. *Electrical Properties of Polymers*, 2nd edn.; Cambridge University Press: New York, NY, 2005.
(60) Resta, R.; Vanderbilt, D. *Theory of Polarization: A Modern Approach*; Springer Berlin Heidelberg: Berlin, Heidelberg, 2007; Vol. *105*, pp 31−68.
(61) DiBenedetto, S. A.; Frattarelli, D. L.; Facchetti, A.; Ratner, M. A.; Marks, T. J. *J. Am. Chem. Soc.* **2009**, *131*, 11080−11090.
(62) Liu, J.; Hennek, J. W.; Buchholz, D. B.; Ha, Y.-G.; Xie, S.; Dravid, V. P.; Chang, R. P. H.; Facchetti, A.; Marks, T. J. *Adv. Mater. Weinheim* **2011**, *23*, 992−997.